Available online at www.sciencedirect.com
ScienceDirect
Journal of the European Ceramic Society 30 (2010) 933–940
www.elsevier.com/locate/jeurceramsoc

New glass and glass–ceramic sealants for planar solid oxide fuel cells

F. Smeacetto [a,*], M. Salvo [a], F.D. D'Hérin Bytner [a], P. Leone [b], M. Ferraris [a]

[a] Department of Materials Science and Chemical Engineering, Politecnico di Torino, Corso Duca degli Abruzzi 24, 10129 Torino, Italy
[b] Department of Energetics, Corso Duca degli Abruzzi 24, 10129 Turin, Italy

Received 15 June 2009; received in revised form 22 September 2009; accepted 30 September 2009
Available online 31 October 2009

Abstract

This work describes the design of three new glass and glass ceramic compositions to join the ceramic electrolyte (YSZ wafer) to the metallic interconnect (Crofer22APU) in planar SOFC stacks. The designed sealants are low-sodium, barium free and boron-oxide free silica-based glasses.

The sealing process was optimized for the most promising composition and joined Crofer22APU/glass–ceramic sealant/YSZ samples were morphologically characterized and tested for 300 h in humidified hydrogen atmosphere at the fuel cell operating temperature of 800 °C. The study showed that the use of the glass–ceramic was successful in joining the YSZ ceramic electrolyte to the Crofer22APU metallic interconnect and in preventing severe corrosion effects at the Crofer22APU/glass–ceramic interface after static treatments in humidified hydrogen at 800 °C for 300 h.

Keywords: Glass–ceramics; Fuel cell; Joining; Sealant

1. Introduction

Solid oxide fuel cells (SOFCs) are highly efficient energy conversion devices which produce electricity by the electrochemical reaction between fuel and an oxidant.[1,2]

One important challenge in the fabrication and commercialization of planar SOFCs is related to the development of sealant materials that must be thermo-mechanically and thermo-chemically stable in both oxidizing and wet-reducing environments at 800 °C for long-term exposures.[3–6]

A critical point in the fabrication of planar SOFCs is the sealing of the electrolyte (yttria-stabilized zirconia wafer or anode-supported, depending on the cell configuration) with the metallic interconnect, in order to obtain a hermetic (gas tight) joint.[7]

There are a number of possible joining or sealing techniques: brazing and sealing with glasses, glass–ceramics and glass-composite seals. Glasses and glass–ceramics show better resistance to the severe service environment (both oxidizing and reducing) than brazing alloys, and depending on the glass composition, they can meet most of the requirements that need to be exhibited by the ideal sealant material.[8–16]

Glass–ceramics that can be prepared by controlled sintering and crystallization of glasses have higher mechanical properties and higher viscosity than glasses at the SOFC operating temperature. Furthermore, glass–ceramics can have thermal expansion coefficients very different from the parent glass, due to the different crystalline phases and their relative proportions.[17–25] In order to develop a suitable glass–ceramic sealant, it is therefore necessary to understand the crystallization kinetics, the sealing properties and the chemical interactions when in contact with other components of the cell.[26,27] Many authors report studies on barium aluminosilicate sealants; these sealants have shown high reactivity with the metallic interconnect at 800–900 °C forming a porous and weak interface composed of barium chromate ($BaCrO_4$) and monocelsian ($BaAl_2Si_2O_8$)[28,29]; aluminization by aerosol spraying of the Crofer22APU surface has been reported to be a viable approach to prevent adverse reaction between Cr-containing metallic interconnects and alkaline-earth silicate sealing glasses containing Ba or Sr.[30]

Concerning other glass compositions, phosphate and borate glasses are not sufficiently stable in a humidified fuel gas environment.[31]

In previous works,[4,5,7] the authors proposed a silica-based, barium and boron free glass–ceramic sealant and discussed its performance in oxidizing and reducing conditions at the fuel cell operating temperature.

* Corresponding author. Tel.: +39 0115644706; fax: +39 0115644699.
E-mail address: federico.smeacetto@polito.it (F. Smeacetto).

0955-2219/$ – see front matter © 2009 Elsevier Ltd. All rights reserved.
doi:10.1016/j.jeurceramsoc.2009.09.033

In the work reported here, new glass and glass–ceramic compositions were designed and tested. Sealants with a lower amount of sodium oxide, compared to the previous composition proposed by the authors, have been designed and tested in order to obtain barium-, phosphor-, boron-oxide free, low-sodium oxide sealant, with thermal expansion coefficient compatible with the metallic interconnect and the electrolyte.

In addition, the joined samples were submitted to thermal ageing tests for 300 h in H_2–3 vol.% H_2O atmosphere at the fuel cell operating temperature of 800 °C. This paper describes the interaction of a new glass–ceramic sealant with Crofer22APU and YSZ at 800 °C, after exposure to reducing conditions (H_2–3 vol.% H_2O atmosphere).

The investigation proposed in this work, can be considered as a preliminary study on the glass–ceramic sealant performance; this glass–ceramic exhibited good performance in humidified hydrogen atmosphere, taking in account that the target operational life of the fuel cell should be thousand of hours and survive at multiple thermal cycles (RT-800 °C).

2. Experimental

The heat resistant metal alloy used as interconnect for this work was Crofer22APU (manufactured by ThyssenKrupp, Germany, production year 2005) containing 22 wt.% chromium and exhibiting a thermal expansion coefficient of 11.5×10^{-6} °C (RT-700 °C). The Crofer22APU was pre-oxidized as described in Ref.[1]. The yttria 8 mol% zirconia wafer (with a thermal expansion coefficient of 10.5×10^{-6} °C, RT-800 °C) had a thickness of 200 μm. The YSZ were supplied by HT Ceramix (Switzerland). The Crofer22APU and YSZ samples to be joined were cut to dimensions: 5 mm × 5 mm.

The three sealant compositions are reported in Table 1 (compositional range of the glass–ceramic sealant previously proposed by the authors, labelled as SACN, is reported for comparison purpose).

The sealants (labelled as SACNMg, SACNLZ and SACNZn) were produced as glasses by melting the appropriate oxides and carbonates raw materials in different proportions and by heating at 1500 °C for 1 h in a platinum crucible; the melt was cast on a brass plate and the transparent glasses were ground for differential thermal analysis (DTA) (Netzsch, Eos) and hot stage microscopy (HSM) experiments (Leitz GmbHAII).

The glasses were powdered and sieved into three different size ranges: <38, 38–75 and >75 μm. The characteristic temperatures of the three compositions were measured by DTA and heating stage microscopy. The thermal behaviour of the glass powder as a function of the particle size by DTA was analysed only for SACNZn. DTA scans were recorded from room temperature to 1100 °C at heating rate of 20 °C/min. Coefficients of thermal expansion were measured on glass and glass–ceramic bars (5 mm × 5 mm × 4 mm, prepared from glass powders sintered at 950 °C for 30 min with a heating rate of 20 °C/min) in a PerkinElmer Thermomechanical Analyser, TMA (heating rate 5 °C/min).

A method for obtaining viscosity–temperature data for the glasses was provided on the basis of the characteristic points obtained by hot stage microscopy.[32]

The glass powders sieved at <38 μm were uniaxial pressed in order to obtain a cubic shape (pellet). A side view hot stage microscope (HSM) with image analysis system and electrical furnace, 1500 Leica, was used. The pellet image is projected through a web cam (Optikam 2) onto the recording device. The image analysis system records the sample geometry during heating, heating rate of 20 °C/min. Percentage decrease in the area of the sample images relative to the initial shape of the pellet are calculated through appropriate HSM software (Image Tool 3.1).

Studies of the wettability of the three glass compositions on the Crofer22APU alloy (pre-oxidised at 900 °C in air for 2 h) and on the YSZ wafer were carried out by hot stage microscopy (LEITZ WETZLAR, Germany) or in a tubular oven under air or Ar atmosphere. HSM data (temperature values) are obtained with an error of ±10 °C; log η (dPa s) values are obtained with an error of ±0.1.

The joined samples were obtained by placing the Crofer22APU plates on YSZ surface with the glass slurry (a mixture of glass powder <38 μm, dispersed in ethanol with solid content 40 wt.%) sandwiched in between. Reproducible results, in terms of joint thickness and homogeneity were obtained on at least six samples. The joining thermal treatment was carried out from room temperature to 950 °C with a dwelling time of 30 min at 950 °C and a heating rate of 20 °C/min, without applying any load.

Heat treatments were performed in a tubular oven (Ar or air atmosphere) at a temperature above the glass softening point, depending on glass composition (T_g + K, where K about 150–200 °C).

The crystalline phase composition of the sealant materials after heat treatment was determined by X-ray diffraction (XRD) analysis. The XRD measurements were conducted on glass–ceramics coated Crofer22APU samples, prepared at 950 °C for 30 min with a heating rate of 20 °C/min, in order to simulate the joining process, without the presence of YSZ on top. It was verified (SEM and XRD) that the crystalline phases were identical on this XRD-sample and the samples covered by YSZ.

Table 1
Sealant compositions (wt.%).

Compositions (wt.%)	SiO_2	Al_2O_3	CaO	MgO	Na_2O	La_2O_3	ZnO
SACNMg	42.2	21.4	34.8	0.3	1.3	–	–
SACNLZ	32.3	17.1	34.2	–	5.7	5	5.7
SACNZn	38.4	19.4	31.6	0.27	1.2	–	9.1
SACN	50–55	10–14	20–25	–	9–12	–	–

Table 2
Characteristic temperatures and coefficients of thermal expansion of the sealants.

Characteristic temperatures	T_g (°C)	Crystallization temperatures (°C)	CTE (°C^{-1}) (200–400 °C)	CTE (°C^{-1}) (RT-800 °C) after crystallization
SACNMg	780	–	8.1×10^{-6}	–
SACNLZ	700	$T_{x1} = 780$; $T_{x2} = 900$	9.7×10^{-6}	–
SACNZn	740	T_x (950–1020)	7.8×10^{-6}	10.0×10^{-6}

Some SACNZn glass–ceramic coated Crofer22APU samples were submitted to HF (4 vol.%) etching for 1 min and examined by SEM.

Joined Crofer22APU/SACNZn/YSZ samples were exposed to H_2–3 vol.% H_2O atmosphere (800 °C for 300 h). The reducing mixture (H_2–3 vol.% H_2O) was obtained by using pure H_2 gas, which was humidified by passing over a water bath kept at a constant temperature of 22.8 °C. The heating rate was 30 °C/h and the dwelling time at 800 °C was 300 h.

Cross-sections of joined samples after the tests were characterized by SEM (Philips 525M) after polishing. EDS (SW9100 EDAX) analysis was carried out in order to detect any elemental diffusion into the sealant before and after H_2–3 vol.% H_2O atmosphere exposure (800 °C for 300 h) and to study the chemical interactions of Crofer22APU, with the glass–ceramic sealant at 800 °C under reducing conditions.

3. Results and discussion

Table 2 summarizes the characteristic temperatures and the thermo-mechanical properties for the three sealants: the sodium oxide content of a previous sealant (9–12 wt.%)[4,5,7] was partially replaced by MgO, La_2O_3 and ZnO as discussed in Section 1.

3.1. SACNMg

Fig. 1 (curve a) shows the viscosity–temperature curve for SACNMg obtained from HSM characteristic points; the glass pellet (glass size < 38 μm) has a log $\eta = 5.5$ at 950 °C (chosen as joining thermal treatment temperature). This thermal treatment was found to be suitable to achieve a good bonding with the substrates (both Crofer22APU and YSZ) without additional external pressure. Moreover, at 800 °C (SOFC operating temperature) the viscosity of the glass pellet is high enough (log $\eta = 9.5$ at 800 °C) to preserve the integrity of the joint.

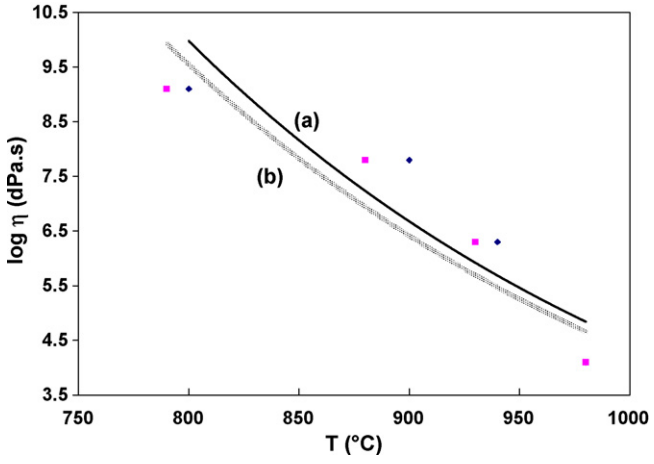

Fig. 1. The viscosity–temperature curves obtained from HSM characteristic viscosity points: (curve a) SACNMg; (curve b) SACNZn.

Lowering sodium content, as expected, led to a glassy material with higher characteristic temperatures. The wettability of SACNMg on Crofer22APU and cubic zirconia was still very high and the sealant/substrate interfaces were continuous and free of pores (Fig. 2a and b). After the heat treatment at 950 °C for 30 min, chosen to join YSZ to Crofer22APU, the SACNMg appeared mostly amorphous (Fig. 2a and b). This is consistent with the low Na_2O amount and with the presence of another network modifier (MgO). The thermal expansion coefficient of as prepared SACNMg, measured by TMA, was 8.1×10^{-6} °C^{-1} (200–400 °C).

Accordingly, SACNMg was not effective as sealant material, because of the formation of cracks parallel to the interfaces with Crofer22APU and YSZ, due to the severe CTE mismatch with components to be joined. Moreover, the mostly amorphous state of SACNMg makes it intrinsically brittle.

3.2. SACNLZ

In order to obtain a higher CTE and to promote devitrification of the sealant, La_2O_3 and ZnO were added into the sealant composition (referred to as SACNLZ). The effect of lanthanum oxide on glass CTE is reported to be similar to that of SrO or BaO.[16] The introduction of lanthanum oxide and zinc oxide determined the devitrification of the parent glass (during the heat treatment necessary for joining process) into a glass–ceramic with a higher CTE with respect to SACNMg glass.

The CTE of the SACNLZ glass was measured to be 9.7×10^{-6} °C^{-1} (200–400 °C; Table 2).

The XRD analysis of the glass–ceramic sealant revealed the presence of calcium zinc aluminum silicate, sodium aluminum silicate and calcium silicate.

Nevertheless, its wetting and sintering capability at 950 °C with Crofer22APU were found not sufficient: HSM experiments showed a scarce sintering capability and softening of SACNLZ at this temperature.

In fact, the viscosity–temperature curve was impossible to obtain from HSM characteristic points since *T* half ball was not detected (up to 1000 °C), due the low amount of glassy phase.

Fig. 2c shows a SEM cross-section of Crofer22APU/SACNLZ/YSZ joined sample; large pores in the glass–ceramic together with a poor adhesion at the Crofer22APU/glass–ceramic sealant can be observed.

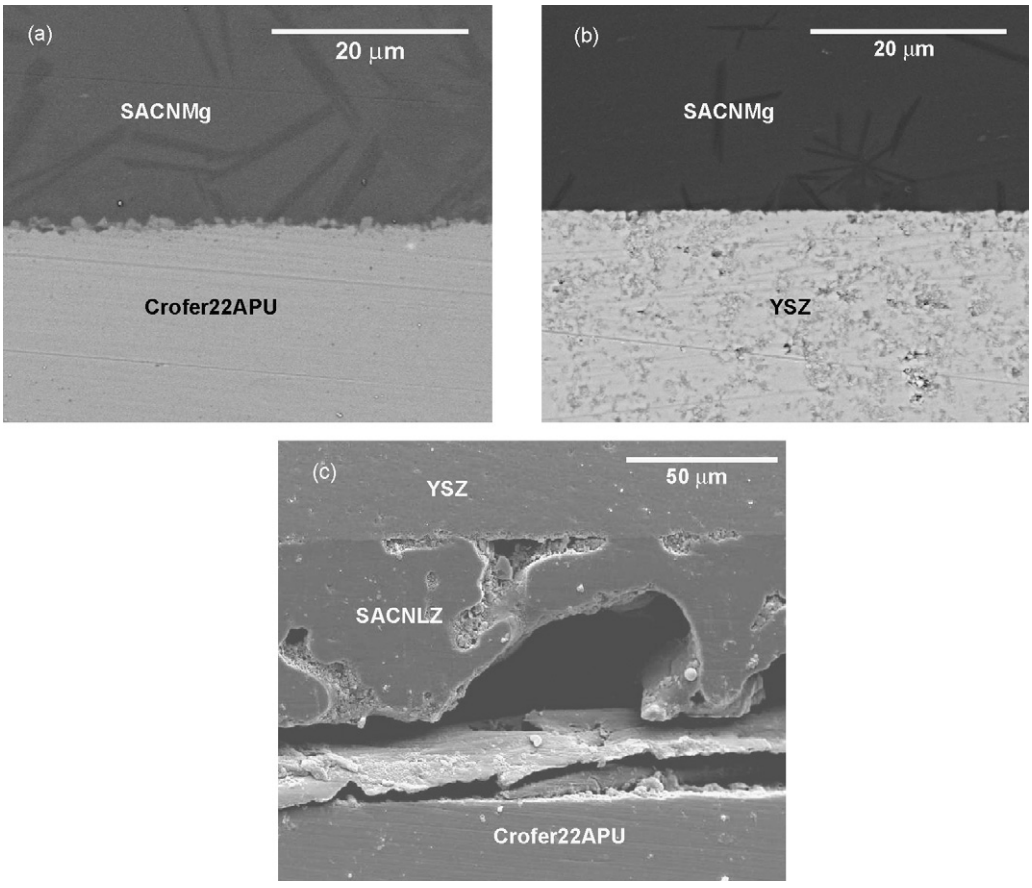

Fig. 2. (a) SEM micrograph of Crofer22APU/SACNMg interface. (b) SEM micrograph of YSZ/SACNMg interface. (c) SEM cross-section of a Crofer22APU/SACNLZ/YSZ joined sample.

3.3. SACNZn

A third sealant composition (referred to as SACNZn), designed to increase CTE and to promote devitrification after joining, was prepared starting from the SACNMg composition and by adding ZnO up to 10 wt.%. In alkaline-earth aluminosilicate glasses the addition of ZnO has been found to decrease the viscosity in the T_g range, while at the same time to slightly increase CTE.[16] Compared to the previous composition, the introduction of zinc oxide up to 10 wt.% determined the devitrification of the parent glass during the heat treatment necessary for joining process into a glass–ceramic with a higher CTE and with a lower viscosity at the joining process temperature.

The further discussion will be concentrated on this glass ceramic sealant.

Fig. 3 shows the DTA curves (heating rate 20 °C/min) of SACNZn glass powders sieved at three different mean particle size ranges and of bulk glass (curve (1) <38 μm, curve (2) mean size between 38 and 75 μm, curve (3) >75 μm, curve (4) bulk glass). The T_g is found to be at 740 °C and an exothermic peak can be detected at higher temperatures. The crystallization peak is considerably affected by the particle size; this peak is shifted to lower temperatures when decreasing the particle size, suggesting a possible effect associated with surface crystallization of the glass, i.e. the crystalline phase formation starts mainly on the surface of the glass particles. The DTA of the bulk glass (curve 4) does not show any crystallization peak before 1000 °C.

Temperatures corresponding to the characteristic viscosity points of the glass pellet were determined by HSM experiments.[32] Fig. 4 shows the pellet images during heat-

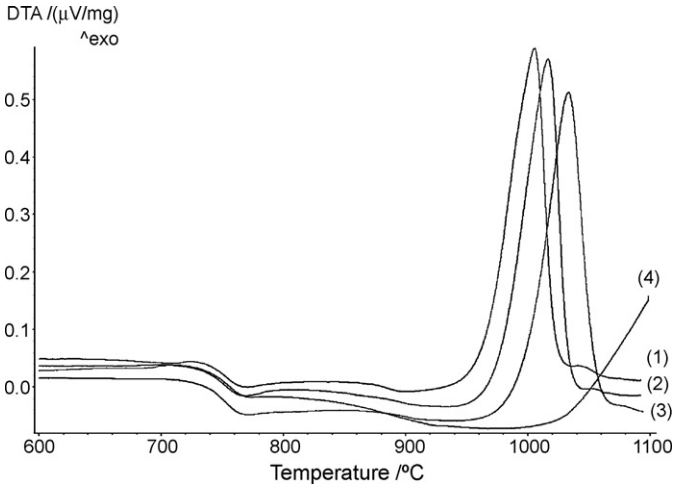

Fig. 3. DTA curves (heating rate 20 °C/min) of SACNZn glass powders at different mean particle size range: curve (1) <38 μm, curve (2) mean size between 38 and 75 μm, curve (3) >75 μm, and curve (4) bulk glass.

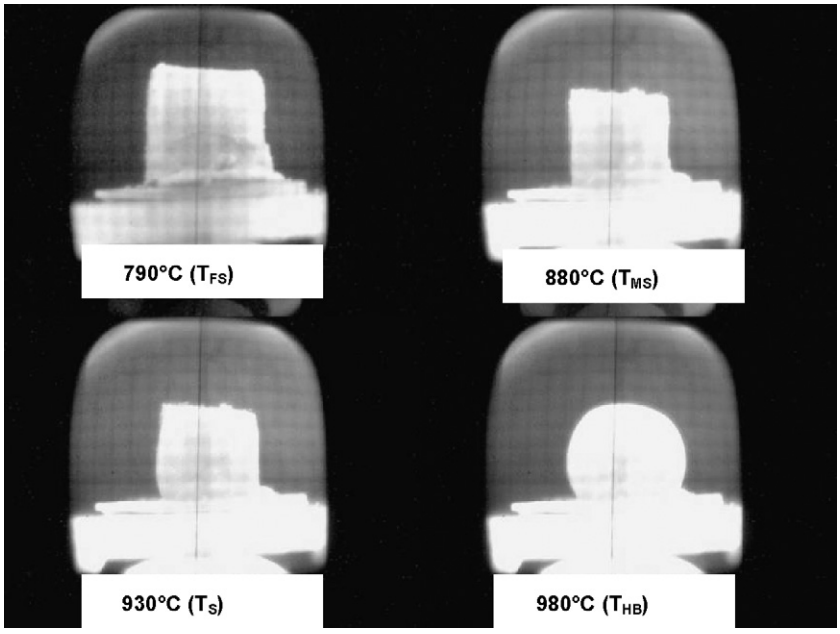

Fig. 4. SACNZn glass pellet images at characteristic viscosity points deduced from HSM experiments.

ing, corresponding to first shrinkage (T_{FS}), maximum shrinkage (T_{MS}), softening (T_R) and half ball (T_{HB}) temperatures respectively.

Fig. 1 (curve b) shows the viscosity–temperature curve obtained from HSM characteristic points for SACNZn; the glass pellet (glass size < 38 μm) has a log $\eta = 5$ at 950 °C (chosen as joining thermal treatment temperature). This thermal treatment was found to be suitable to achieve a good joining of the substrates (both Crofer22APU and YSZ) without additional external pressure. Besides, at 800 °C (SOFC operating temperature) the viscosity of the glass pellet is high enough (log $\eta = 9$ at 800 °C) to preserve the integrity of the joint. Furthermore, the crystallization occurring during the thermal treatment of the joining process promotes a further increase in the viscosity of the joint at this temperature.

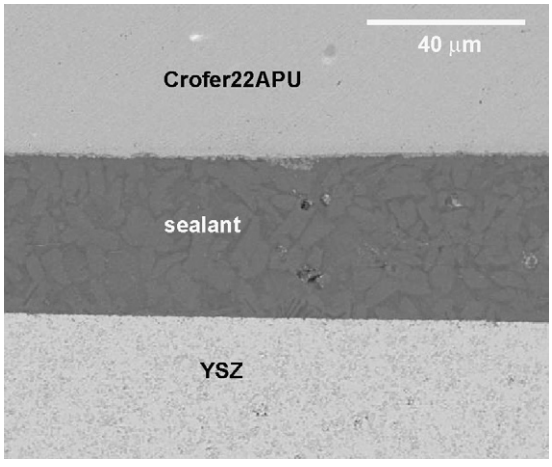

Fig. 5. SEM micrograph of a Crofer22APU/SACNZn glass–ceramic sealant/YSZ cross-section.

Fig. 5 shows a SEM micrograph of a Crofer22APU/SACNZn glass–ceramic sealant/YSZ cross-section. The joint region has an average thickness of 50 μm. Examination around the joining region shows that very low residual porosity is present, indicating that this sealant should provide high gas tightness and a hermetic structure. A very good adhesion between the glass–ceramic and both Crofer22APU and YSZ can be observed. The absence of cracks near the interface of the glass ceramic with both Crofer22APU and YSZ demonstrates their good physical compatibility with the glass–ceramic sealant. The as produced glass has a thermal expansion coefficient of $7.8 \times 10^{-6}\ K^{-1}$ (200–400 °C), while the glass–ceramic, obtained after the heat tretament necessary for joining process, has a thermal expansion coefficient of $10.0 \times 10^{-6}\ K^{-1}$ (RT-800 °C).

The XRD pattern of the SACNZn glass–ceramic sealant reported in Fig. 6 revealed the presence of calcium zinc aluminum silicate ($Al_{1.25}Ca_{1.94}O_7Si_{1.38}Zn_{0.43}$) and sodium calcium aluminum silicate ($Al_{1.2}Ca_{0.2}Na_{0.8}O_8Si_{2.8}$), moreover a

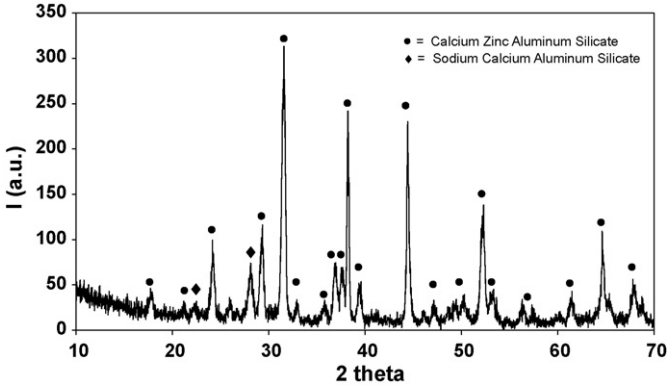

Fig. 6. XRD pattern of the SACNZn glass–ceramic sealant.

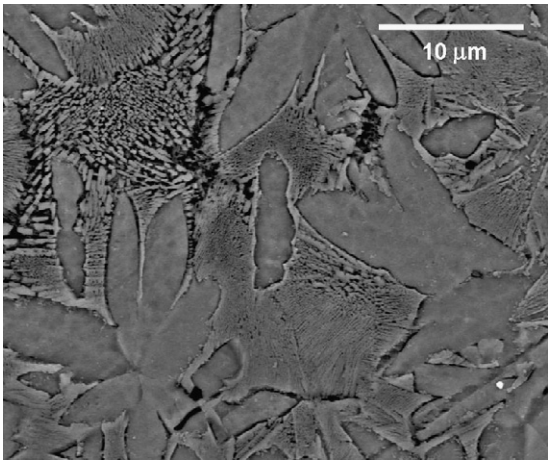

Fig. 7. SEM top view of the SACNZn glass–ceramic sealant.

high degree of crystallization can be observed. The high degree of crystallization (as detected by XRD and SEM) of the SACNZn after crystallization at 950 °C (Tx for SACNZn with glass powder size lower than 38 μm) could be due to the long dwelling time (1 h) and high nucleation rate. At this purpose, it must be highlighted that a high degree of crystallization is desirable to increase thermo-mechanical properties of the sealant (i.e. stability) and to prevent substantial microstructural modification during SOFC operation at high temperatures (up to 900 °C).

A top view of the HF etched SACNZn glass–ceramic sealant (back scattered electron image) is shown in Fig. 7; the glass–ceramic sealant exhibits a fairly homogeneous microstructure. Two crystalline phases are visible, embedded in a glassy matrix (HF etched phase).

Fig. 8a is a magnification of the interface zone between the glass–ceramic and the YSZ. The interface is continuous and without pores or cracks. Fig. 8b shows a detail of the Crofer22APU/glass–ceramic sealant interface. The pre-oxidation layer (chromium–manganese oxide scale) is clearly visible. The glass–ceramic adhered well to the pre-oxidised Crofer22APU and a defect free structure, without voids and microcracks, can be observed.

After a mid-term exposure (300 h at 800 °C) of Crofer22APU/SACNZnglass ceramic/YSZ samples in a reducing atmosphere (H_2–3 vol.% H_2O), it was observed that the samples and seal region remained intact. Fig. 9 shows a SEM cross-section of the of Crofer22APU/SACNZn glass ceramic sample after 300 h of exposure to H_2–3 vol.% H_2O atmosphere. The SEM micrograph is focused on the central part of the joined sample. It is evident that no interfacial delamination at the glass–ceramic/steel interface took place. It can be also observed that the joint region does not exhibit any substantial modification from the morphological point of view. No cracks or pores are present, and the interface between the glass–ceramic and the Crofer22APU is still free of cracks and continuous.

Fig. 9 shows also elemental maps of Fe, Na, Zn, Mn, Cr and O; it is evident that there is no reaction between the chromium–manganese oxide scale (white arrow) and the glass ceramic components and consequently no new products at the Crofer22APU/glass–ceramic interface were found; moreover, there was no reaction of the elements in the glass–ceramic with chromium and no sodium chromate formation, which is undesirable.[13] These data showed no migration of sodium away from the SACNZn glass–ceramic sealant which maintained good adhesion to the Crofer22APU substrate.

At this purpose, it must be highlighted that Na (as discussed above) was found to be predominant in one of the two crystalline phases. This could explain the higher thermodynamic stability of this glass–ceramic sealant, compared to other glassy sealants containing sodium, where severe corrosion was observed.[5,33,34]

This observation is confirmed by the experimental observation of no undesired reactions taking place and no corrosion products formed at the Crofer22APU–SACNZn glass–ceramic sealant interface during exposure to the H_2–3 vol.% H_2O atmosphere.

Fig. 10 is a SEM image of the interface between the SACNZn glass–ceramic and YSZ showing that also this interface is still free of pores and cracks after heat treatment at 800 °C under humidified hydrogen atmosphere; moreover the glass–ceramic sealant did not exhibit microstructural modification. An EDS line scan analysis revealed no diffusion of yttrium from YSZ into the glass–ceramic. This result confirmed the thermo-chemical compatibility of the SACNZn glass–ceramic sealant and YSZ at 800 °C under humidified hydrogen atmosphere.

According to the preliminary experimental tests, the SACNZn glass–ceramic can be considered as a candidate sealant between the YSZ electrolyte and the Crofer22APU intercon-

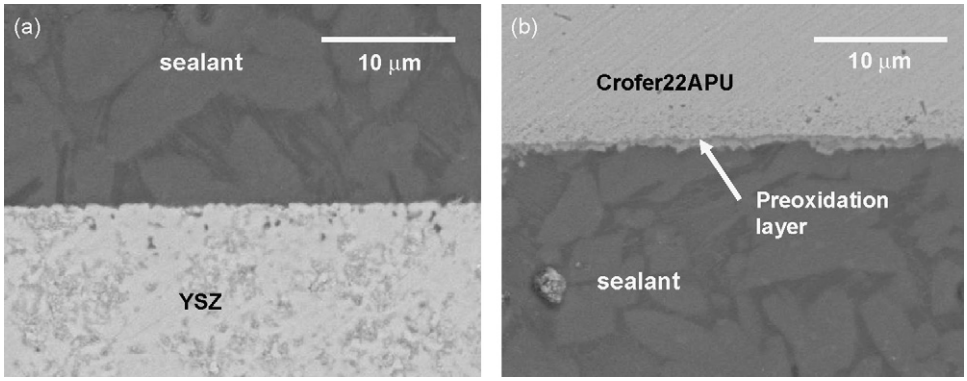

Fig. 8. (a) SEM micrograph of interface zone between the SACNZn glass–ceramic and the YSZ and (b) SEM micrograph detail of the Crofer22APU/SACNZn glass–ceramic sealant interface.

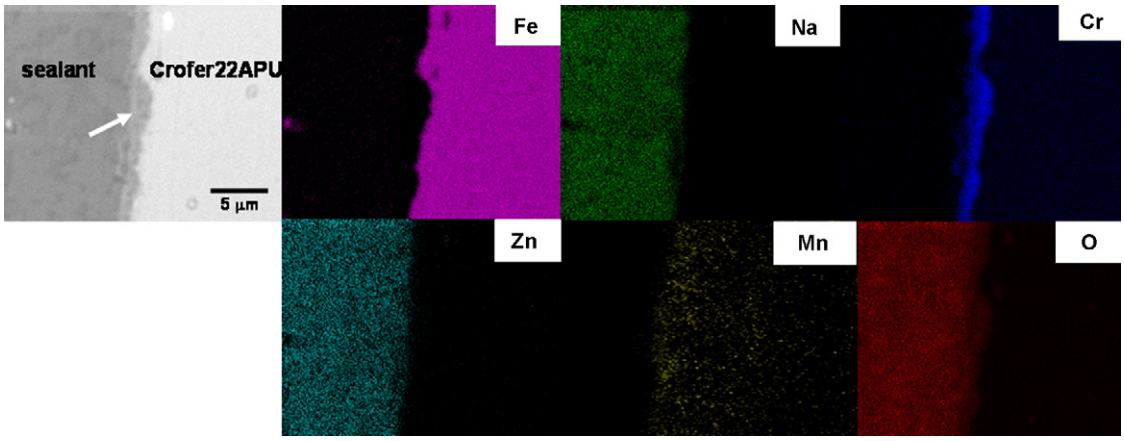

Fig. 9. SEM cross-section of the of Crofer22APU/SACNZn glass ceramic sample after 300 h of exposure (at 800 °C) to H_2–3 vol.% H_2O atmosphere and relative elemental maps of Fe, Na, Zn, Mn, Cr and O.

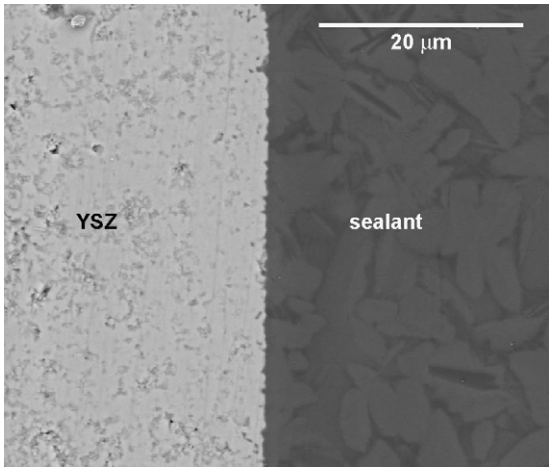

Fig. 10. SEM micrograph of the YSZ/SACNZn glass–ceramic interface after 300 h of exposure (at 800 °C) to H_2–3 vol.% H_2O atmosphere.

nect. In order to qualify this glass–ceramic as sealant between interconnect plates, electrical properties should be measured and provided for a further study in order to improve and complete its characterization.

4. Conclusions

This work proposed the design, development and performance of a new low-sodium, barium and boron free silica-based glass–ceramic sealant used to join the ceramic electrolyte (YSZ wafer) to the metallic interconnect (Crofer22APU) in planar SOFC stacks.

A detailed characterization of three proposed sealants was carried out. A preliminary study on the most promising glass–ceramic sealant showed that after static treatments in humidified hydrogen at 800 °C for 300 h the glass–ceramic was successful in preventing adverse corrosion effects at the Crofer22APU/glass–ceramic sealant interfaces. The SACNZn glass ceramic sealant exhibited a promising behaviour in humidified hydrogen atmosphere if compared to the other glass composition previously published by the authors (where both oxidizing and reducing conditions were tested, up to 500 h); at this purpose, in order to have a more detailed characterization of the SACNZn glass–ceramic sealant, further studies will be addressed to multiple thermal cycling (RT-800 °C), in order to evaluate the thermo-mechanical resistance of the Crofer22APU/SACNZn/YSZ joined samples.

Acknowledgments

The authors gratefully acknowledge the help of HTCeramix for supplying the Crofer22 APU interconnect and electrolyte materials for the study. The contribution to the experimental work of Ms. Sara Marchisio, graduate student on Materials Engineering at Politecnico di Torino is kindly acknowledged.

This work was supported in part by EU Network of Excellence project Knowledge-based Multicomponent Materials for Durable and Safe Performance (KMM-NoE, NMP3-CT-2004-502243) and MULTISS: “Design and in-house development of SOFC stacks for dealing with multiple fuels” (Regione Piemonte project, Italy).

References

1. Steele, B. C. H. and Heinzel, A., Materials for fuel-cell technologies. *Nature*, 2001, **414**, 345–352.
2. Singh, R. N., Sealing technology for solid oxide fuel cells (SOFC). *International Journal of Applied Ceramic Technology*, 2007, **4**, 134–144.
3. Yokokawa, H., Tu, H., Iwanschitz, B. and Mai, A., Fundamental mechanisms limiting solid oxide fuel cell durability. *Journal of Power Sources*, 2008, **182**, 400–412.
4. Smeacetto, F., Salvo, M., Ferraris, M., Cho, J. and Boccaccini, A. R., Glass–ceramic seal to join Crofer 22 APU alloy to YSZ ceramic in planar SOFCs. *Journal of the European Ceramic Society*, 2008, **28**, 61–68.
5. Smeacetto, F., Chrysanthou, A., Salvo, M., Zhang, Z. and Ferraris, M., Performance and testing of glass–ceramic sealant used to join anode-supported-electrolyte to Crofer22APU in planar solid oxide fuel cells. *Journal of Power Sources*, 2009, **190**, 402–407.
6. Deng, X., Duquette, J. and Petric, A., Silver–glass composite for high temperature sealing. *International Journal of Applied Ceramic Technology*, 2007, **4**, 145–151.
7. Smeacetto, F., Salvo, M., Ferraris, M., Casalegno, V. and Asinari, P., Glass and composite seals for the joining of YSZ to metallic interconnect in solid oxide fuel cells. *Journal of the European Ceramic Society*, 2008, **28**, 611–616.

8. Zhou, X., Sun, K., Yan, Y., Le, S., Zhang, N., Sun, W. *et al.*, Investigation on silver electric adhesive doped with Al_2O_3 ceramic particles for sealing planar SOFC. *Journal of Power Sources*, 2009, **192**, 408–413.
9. Kuhn, B., Wetzel, F. J., Malzbender, J., Steinbrech, R. W. and Singheiser, L., Mechanical performance of reactive-air-brazed (RAB) ceramic/metal joints for solid oxide fuel cells at ambient temperature. *Journal of Power Sources*, 2009, **193**, 199–202.
10. Story, C., Lu, K., Reynolds, W. T. and Brown, D., Shape memory alloy/glass composite seal for solid oxide electrolyzer and fuel cells. *International Journal of Hydrogen Energy*, 2008, **33**, 3970–3975.
11. Singh, M., Shpargel, T. P. and Asthana, R., Brazing of stainless steel to yttria-stabilized zirconia using gold-based brazes for solid oxide fuel cell applications. *International Journal of Applied Ceramic Technology*, 2007, **4**, 119–133.
12. Le, S., Sun, K., Zhang, N., Shao, Y., An, M., Fu, Q. *et al.*, Comparison of infiltrated ceramic fiber paper and mica base compressive seals for planar solid oxide fuel cells. *Journal of Power Sources*, 2007, **168**, 447–452.
13. Nielsen, K. A., Solvang, M., Nielsen, S. B. L., Dinesen, A. R., Beeaff, D. and Larsen, P. H., Glass composite seal for SOFC application. *Journal of the European Ceramic Society*, 2007, **27**, 1817–1822.
14. Meinhardt, K. D., Kim, D. S., Chou, Y. S. and Weil, K. S., Synthesis and properties of a barium aluminosilicate solid oxide fuel cell glass–ceramic sealant. *Journal of Power Sources*, 2008, **182**, 188–196.
15. Goel, A., Tulyaganov, D. U., Kharton, V. V., Yaremchenko, A. A., Eriksson, S. and Ferreira, J. M. F., Optimization of La_2O_3-containing diopside based glass–ceramic sealants for fuel cell applications. *Journal of Power Sources*, 2009, **189**, 1032–1043.
16. Flugel, A., Dolan, M., Varshneya, A. K., Zheng, Y., Coleman, N., Hall, M. *et al.*, Development of an improved devitrifiable fuel cell sealing glass. *Journal of the Electrochemical Society*, 2007, **154**, B601–B608.
17. Pascual, M. J., Guillet, A. and Duran, A., Optimization of glass–ceramic sealant compositions in the system MgO–BaO–SiO_2 for solid oxide fuel cells (SOFC). *Journal of Power Sources*, 2007, **169**, 40–46.
18. Wang, R., Lü, Z., Liu, C., Zhu, R., Huang, X., Wei, B. *et al.*, Characteristics of a SiO_2–B_2O_3–Al_2O_3–BaO–PbO_2–ZnO glass–ceramic sealant for SOFCs. *Journal of Alloys Compounds*, 2007, **432**, 189–193.
19. Gosh, S., Kundu, P., Das Sharma, A., Basu, R. N. and Maiti, H. S., Microstructure and property evaluation of barium aluminosilicate glass–ceramic sealant for anode-supported solid oxide fuel cell. *Journal of the European Ceramic Society*, 2008, **28**, 69–76.
20. Laorodphan, N., Namwong, P., Thiemsorn, W., Jaimasith, M., Wannagon, A. and Chairuangsri, T., A low silica, barium borate glass–ceramic for use as seals in planar SOFCs. *Journal of Non-Crystalline Solids*, 2009, **355**, 38–44.
21. Zhang, T., Brow, R. K., Reis, S. T. and Ray, C. S., Isothermal Crystallization of a solid oxide fuel cell sealing glass by differential thermal analysis. *Journal of the American Ceramic Society*, 2008, **91**, 3235–3239.
22. Stephens, E. V., Vetrano, J. S., Koeppel, B. J., Chou, Y., Sun, X. and Khaleel, M. A., Experimental characterization of glass–ceramic seal properties and their constitutive implementation in SOFC stack models. *Journal of Power Sources*, 2009, **193**, 625–631.
23. Liu, W., Sun, X. and Khaleel, M. A., Predicting Young's modulus of glass/ceramic sealant for solid oxide fuel cell considering the combined effects of aging, micro-voids and self-healing. *Journal of Power Sources*, 2008, **185**, 1193–1200.
24. Goel, A., Tulyaganov, D. U., Goel, I. K., Shaaban, E. R. and Ferreira, J. M. F., Effect of BaO on the crystallization kinetics of glasses along the diopside–Ca-Tschermak join. *Journal of Non-Crystalline Solids*, 2009, **355**, 193–202.
25. Malzbender, J., Monch, J., Steinbrech, R. W., Koppitz, T., Gross, S. M. and Remmel, J., Symmetric shear test of glass–ceramic sealants at SOFC operation temperature. *Journal of Materials Science*, 2007, **42**, 6297–6301.
26. Lahl, N., Bahadur, D., Singh, K., Singheiser, L. and Hilpertz, K., Chemical interactions between aluminosilicate base sealants and the components on the anode side of solid oxide fuel cells. *Journal of The Electrochemical Society*, 2002, **149**, A607–A614.
27. Menzler, N. H., Sebold, D., Zahid, M., Gross, S. M. and Koppitz, T., Interaction of metallic SOFC interconnect materials with glass–ceramic sealant in various atmosphere. *Journal of Power Sources*, 2005, **152**, 156–167.
28. Batfalsky, P., Haanappel, V. A. C., Malzbender, J., Menzler, N. H., Shemet, V., Vinke, I. C. *et al.*, Chemical interaction between glass–ceramic sealants and interconnect steels in SOFC stacks. *Journal of Power Sources*, 2006, **155**, 128–137.
29. Chou, Y. S., Stevenson, J. W. and Gow, R. N., Novel alkaline earth silicate sealing glass for SOFC Part II. Sealing and interfacial microstructure. *Journal of Power Sources*, 2007, **170**, 395–400.
30. Chou, Y. S., Stevenson, J. W. and Sing, P., Effect of aluminizing of Cr-containing ferritic alloys on the seal strength of a novel high-temperature solid oxide fuel cell sealing glass. *Journal of Power Sources*, 2008, **185**, 1001–1008.
31. Larsen, P. H., Poulsen, F. W. and Berg, R. W., The influence of SiO_2 addition to 2MgO–Al_2O_3–3.3P_2O_5 glass. *Journal of Non-Crystalline Solids*, 1999, **244**, 16–24.
32. Pascual, M. J., Durán, A. and Prado, M. O., A new method for determining fixed viscosity points of glasses. *Physics and Chemistry of Glasses*, 2005, **46**, 512–520.
33. Horita, T., Kshimoto, H., Yamaji, K., Sakai, N., Xiong, Y., Brito, M. E. *et al.*, Anomalous oxidation of ferritic interconnects in solid oxide fuel cells. *International Journal of Hydrogen Energy*, 2008, **33**, 3962–3969.
34. Ogasawara, K., Kameda, H., Matsuzaki, Y., Sakurai, T., Uehara, T., Toji, A. *et al.*, Chemical stability of ferritic alloy interconnect for SOFCs. *Journal of the Electrochemical Society*, 2007, **154**, B657–B663.